SAND2011-2589P

Gaseous Hydrogen Embrittlement of High Performance Metals in Energy Systems

Editors: R.P. Gangloff, B.P. Somerday

Chapter 3.7 Austenitic Stainless Steels

Chris San Marchi
Sandia National Laboratories, Livermore, CA, USA

Abstract

This chapter reviews the current state of understanding of hydrogen-assisted deformation and fracture of austenitic stainless steels for use in gaseous hydrogen. The basic characteristics of austenitic stainless steels are presented, focusing on the alloys most commonly used in gaseous hydrogen service. Hydrogen transport in austenitic alloys is briefly discussed, followed by a summary of the important characteristics of internal and external hydrogen environments. A few brief comments are given on models of hydrogen-assisted deformation and fracture with emphasis on hydrogen-enhanced localized plasticity. Observations of fracture are summarized for austenitic stainless in the presence of hydrogen and related to the tendency for localized deformation in this material class. In the following section, the basic trends of hydrogen-assisted deformation and fracture are outlined with examples from the literature for tensile, fracture and fatigue testing, respectively. In concluding, necessary research and development activities are mentioned throughout the text are summarized in the context of unambiguously elucidating the micromechanisms of hydrogen-assisted fracture in austenitic stainless steels.

3.7.1 Introduction

This chapter aims to provide a brief overview of hydrogen-assisted deformation and fracture in austenitic stainless steels in the context of exposure to gaseous hydrogen. Ferritic and martensitic stainless steels are not considered in this chapter since their behavior in gaseous hydrogen is similar to other high-strength steels as covered in the chapters by Garrison and Moody, and McMahon of this volume, as well as elsewhere [1]; moreover, ferritic and martensitic stainless steels are generally not appropriate for use in high-pressure gaseous hydrogen.

Austenitic stainless steels are commonly employed for their corrosion resistance, high ductility and toughness, and low ductile-to-brittle transition temperature. This class of material is particularly important for the petrochemical industry and for gas-handling equipment, including installations for delivering gaseous hydrogen as a fuel. Consequently, austenitic stainless steels in a variety of product forms (tubing, valve bodies, pressure vessels, etc) have extensive service history in gaseous hydrogen [2]. Hydrogen-assisted fracture of austenitic stainless steels has also been extensively studied; see, for example, the several prominent reviews [3-8]. This overview does not try to review all of the literature on the effects of gaseous hydrogen on austenitic stainless steels; rather, the goal is to provide a critical assessment of the current understanding of hydrogen-assisted deformation and fracture in common austenitic stainless steels. In particular, this overview emphasizes understanding the fundamental modes of deformation and fracture in the presence of gaseous hydrogen with acknowledgement of the role of hydrogen transport within the metal.

3.7.2 Fundamentals of austenitic stainless steels

While austenitic stainless steels can be classified in numerous ways; for the purposes of this review, the focus is common structural alloys that are distinguished by the stability of the alloy with respect to phase transformations during deformation. The distinction between the stable alloys and the metastable alloys is not always clear, since stability depends on the exposure conditions (e.g., temperature and strain). For this review, stable alloys are considered to be those that generally do not form α'-martensite when fractured in uniaxial tension at room temperature (i.e., strain-induced α'-martensite). Stable austenitic stainless steels that have been studied in gaseous hydrogen environments include primarily three alloys: 21Cr-6Ni-9Mn (also referred to by its tradename Nitronic 40 or XM-11), 22Cr-13Ni-5Mn (Nitronic 50 or XM-19), and AISI type 310. AISI type 304 and type 316 (and their many variants) represent the metastable austenitic stainless steels that have been most heavily studied in gaseous hydrogen environments. Precipitation-strengthened austenitic stainless steels represent a third important class of alloys; the most common alloy being A-286 (AISI type 600) [9]. In the context of this overview, modified A-286 [10] (also called JBK-75) is considered to be the same as A-286.

Austenite is distinguished from other common steel phases by its face-centered cubic (FCC) crystal structure. Austenite is non-magnetic and differs from the ferritic phases typical of other steels by its comparatively high solubility for hydrogen and low diffusivity for hydrogen [8]. The primary alloying elements are chromium and nickel, which stabilize the austenitic phase. Nitrogen is also a strong austenite stabilizer that (ideally) remains in solid solution, while manganese is used to increase the solubility of nitrogen and substitute for nickel [9]. Alloying in austenitic stainless steels is particularly important because the allowed compositional range is quite large (e.g., AISI type 304 can have nickel content between 8 and 12 wt%). Since many of

the alloying elements are expensive (particularly nickel, which generally drives the cost of austenitic stainless steels), it is not uncommon for steel mills to produce stainless steels with composition near the lower bound of the allowed compositional ranges, particularly with regard to the expensive elements, such as nickel and molybdenum. There are numerous alloy formulations that significantly reduce (or eliminate) nickel (AISI type 200 series), but this requires additional alloying elements to stabilize the austenitic phase, such as nitrogen and manganese.

There are many variations of the general types of austenitic stainless steels. A low-carbon grade exists for many stainless steels, for example, often designated with an "L" as in type 304L and type 316L. Moreover, multiple compositional parameters may vary from one materials specification to another. The significance of these variations has often been overlooked both in the engineering community and in the scientific literature. The example of type 316 alloys is particularly instructive: although the primary difference between type 316 and type 316L alloys is carbon content, some specifications for type 316L (e.g., SUS 316L, Japanese Industrial Standard) require a minimum of 12 wt% nickel, while materials specifications for type 316 (and 316L) stainless steels from the American Society of Testing and Materials (ASTM) allow as low as 10 wt% nickel. As will be discussed in a subsequent section, this difference in nickel content critically impacts hydrogen-assisted deformation and fraction (Figures 1 and 2). While SUS316L is reported to be more resistant to gaseous hydrogen than type 316, for the same nickel content, SUS316L and type 316 alloys behave similarly (Figure 1). In short, materials designations (such as type 316) are generally insufficient to assess the hydrogen-assisted fracture in austenitic stainless steels.

There are many second phases that can be found in austenitic stainless steels [11] and for the most part, they are undesirable. Austenitic stainless steels, for example, are sensitive to carbide precipitation on grain boundaries between approximately 773 K and 1073 K; this phenomenon is called sensitization. Carbide precipitation in stainless steels depletes the adjacent regions of chromium and carbon, making these areas more prone to general corrosion [9] and vulnerable to deformation-induced phase transformations [12]. Additional second phases can form during primary processing and thermal exposure [11], although sensitization and strain-induced martensite are the most broadly relevant issues in relation to second phases in austenitic stainless steels.

Deformation in metastable austenitic stainless steels can result in the transformation of austenite (γ) to martensite. Two distinct phases of martensite can be formed: ε-martensite has a hexagonal close packed (HCP) crystal structure and is non-magnetic, while α'-martensite is magnetic and has body-centered tetragonal (BCT) crystal structure, but often approximated as body-centered cubic (BCC). ε-martensite can be a precursor to α'-martensite ($\gamma \rightarrow \varepsilon \rightarrow \alpha'$) or α'-martensite can form directly from austenite ($\gamma \rightarrow \alpha'$) [11]. Lower alloy content and lower temperature promote the formation of deformation-induced martensite; carbon and nitrogen are particularly potent austenite stabilizers, while nickel is the most important transition metal for stabilizing austenite [13].

Austenitic stainless steels are used primarily for their corrosion resistance, thus strengthening is often a secondary concern. Nitrogen is one of the few solid-solution elements that impacts strength. Some stable alloys, such as 21Cr-6Ni-9Mn and 22Cr-13Ni-5Mn, display annealed yield strength that is more than 50% greater than the metastable alloys due to their higher nitrogen

content. Austenitic stainless steels can also be strengthened by deformation as these alloys display significant strain hardening. The precipitation-strengthened alloys derive significant strengthening from the controlled precipitation of the γ' phase (coherent Ni_3Ti precipitates) [9]. Martensite is also a potent strengthener in austenitic stainless steel and it has been suggested that this feature can be used for strengthening [14].

Deformation in austenitic stainless steels is influenced by alloy content and temperature. For the purposes of this discussion, the localized plasticity in the form of planar deformation and into deformation (shear) bands is distinguished from uniform deformation, where cross-slip characterizes plasticity. Localized deformation and so-called planar slip are often used interchangeably in the literature, although both homogeneous-planar deformation along discrete slip planes as well as heterogeneous formation of deformation bands are specific manifestations of localized deformation. Nickel content, in particular, strongly affects deformation: for type 316 austenitic stainless steels, deformation is increasingly localized in bands for alloys with lower nickel content [15]. In addition, lower temperature promotes the formation of deformation bands [15]. At high stress, plasticity is dominated by deformation twinning [16-18]. More generally, the propensity to form deformation bands (and deformation twins) scales with lower stacking fault energy (SFE), which is related to composition and temperature [19, 20]. A number of simple linear relationships for SFE with the primary alloying elements are given in the literature [21-23], although the interactions of alloying elements are certainly more complex than these relationships imply. In particular, nickel shows a relatively strong positive effect on SFE. The available evidence suggests that SFE is weakly affected by carbon and nitrogen [23, 24], for relevant carbon contents in austenitic stainless steels and for nitrogen contents typical of metastable alloys. In the stable 21Cr-6Ni-9Mn alloy, higher nitrogen content (>0.2 wt%) lowers

SFE [25]. While SFE is a convenient first-order metric to distinguish the relative character of deformation (localized versus uniform) in austenitic stainless steels, other microstructural characteristics also affect the character of deformation. Ordering and coherent precipitation, for example, promote localization of deformation. As will be described in the following sections, resistance to hydrogen-assisted fracture is related to the character of deformation in austenitic stainless steels, thus it is important to recognize the microstructural variables that influence deformation modes.

3.7.3 Hydrogen transport

The transport of hydrogen in austenitic stainless steels was recently reviewed in Ref. [26] and is described more generally in a separate chapter in this volume. By definition, diffusivity (D) and solubility (K) of hydrogen are thermodynamic parameters that assume hydrogen interacts uniformly with the metal lattice (i.e., not affected by trapping). The permeability of hydrogen (Φ) is simply the product of these two parameters. Both D and K display the classic thermodynamic dependence on temperature as given in Table 1.

Hydrogen can also be trapped by microstructural features, such as grain boundaries, phase boundaries, and dislocations [27-29]. While hydrogen trapping can, in principle, increase the amount of hydrogen in a metal, the concentration of trapped hydrogen is very small compared to the total hydrogen concentration in austenitic stainless steels at equilibrium [30]. Hydrogen trapping near ambient temperature, however, can reduce the apparent diffusivity [26]. The trap binding energy is relatively low in austenitic stainless steels (about 20 kJ/mol) and associated with dislocations [31].

Hydrogen also interacts elastic stress fields in metals: hydrostatic tension increases the volume of the lattice and the concentration of hydrogen, while hydrostatic compression decreases the hydrogen concentration. The relationship that describes this effect [32, 33] is written as

$$c_S / c_L = \exp\left(\frac{V_H \bar{\sigma}}{RT}\right) \tag{1}$$

where c_L is the hydrogen concentration in the unstressed lattice, c_S is the concentration of hydrogen in the lattice subjected to a hydrostatic stress $\bar{\sigma} = \sigma_{ii}/3$, and V_H is the partial molar volume of hydrogen in the lattice, which for steel is on the order of 2 cm^3/mol [28]. The effect of stress on hydrogen dissolved in the lattice is greatest at low temperature (due to the positive exponential term and its inverse proportionality to temperature).

Permeability is nearly independent of the composition and microstructure for austenitic stainless steels that have been tested, including stable [34-36] and metastable alloys [34-38] as well as the precipitation-strengthened A-286 alloy [39]. The solubility, on the other hand, varies with composition [26]. The compositional dependencies are not fully elucidated in the literature, although it has been pointed out that the stable Fe-Cr-Ni-Mn alloys have greater solubility than the metastable Fe-Cr-Ni alloys [26]. Diffusivity varies somewhat with composition of austenitic stainless steels, although this variation is small compared to the diffusivity in other alloy systems, such as the ferritic steels. The diffusivity of lattice hydrogen in austenite at room temperature is on the order of 10^{-16} m^2/s, while for the ferritic steels diffusivity tends to be closer to 10^{-8} m^2/s. This is an important consideration, since strain-induced martensite is essentially a ferritic phase, acting as a rapid path for hydrogen transport [35, 38]. An order of magnitude estimate of diffusion distance x can be determined from

$$x \sim (Dt)^{1/2} \quad (2)$$

where t is time. For one hour of exposure and data from Table 1, equation (2) gives a diffusion distance of about one micrometer for austenitic stainless steels.

The concept of hydrogen transport by glissile dislocations was proposed [40] to explain hydrogen-assisted fracture on relatively short-time scales in austenitic stainless steels. However, experimental evidence to support so-called dislocation transport of hydrogen is relatively limited [41-44]. Review of the very limited experimental data demonstrates that the effective transport distances of hydrogen remain relatively unchanged in stainless steels exposed to gaseous hydrogen during deformation [41]. The magnitude of the hydrogen concentration and hydrogen flux during deformation of austenitic stainless steels also remains comparable to those in the absence of deformation [41, 44]. Although dislocation transport is often assumed in the literature, critical assessments of this interpretation have concluded that hydrogen transport by dislocations is not a requirement for hydrogen-assisted fracture in austenitic stainless steels [41] and does not make a significant contribution to diffusive transport [45]. In contrast, deformation-induced martensite clearly enhances hydrogen transport [35, 38, 45], which may account for the interpretations in some studies that presume transport by dislocations.

The solubility of hydrogen is expected to be approximately the same for hydrogen isotopes, while diffusivity depends on the mass of the isotope. Solubility is dictated by thermodynamic equilibrium and the thermodynamic properties of the individual isotopes, which are nearly identical at ambient and elevated temperature [46-48]. Classical rate theory predicts diffusivity to be inversely proportional to the square root of the mass of the isotope, such that:

$$D_H / D_D = \sqrt{m_D / m_H} \tag{3}$$

where D and m are the diffusivity and mass of the respective isotope, and the subscripts H and D refer to hydrogen and deuterium respectively. Similar expressions can be written for tritium and can be simplified as $D_H = \sqrt{2} D_D = \sqrt{3} D_T$, where the subscript T refers to tritium. Since solubility is presumed independent of isotope, the permeability will have the same dependence on isotope as the diffusivity, as confirmed at elevated temperatures for nickel [49] and stainless steels [50-53].

3.7.4 Environmental test methods

3.7.4.1 External hydrogen

Testing in gaseous hydrogen is desirable because the environmental conditions of interest can be closely replicated. The effects of hydrogen, however, are manifest when external hydrogen diffuses into the metal [5, 54, 55]. Distinguishing intrinsic resistance to hydrogen-assisted fracture, apart from kinetic limits to hydrogen uptake, is challenging. Surface kinetics often control hydrogen uptake and are difficult to quantify, making prediction of hydrogen ingress on short-time scales a particularly challenging task. The challenge associated with surface kinetics is exemplified by diffusion studies, where special attention to surface condition is necessary to quantitatively evaluate transients in hydrogen transport [26].

Hydrogen transport by diffusion is also an important consideration for interpreting testing results. The dependence of hydrogen effects on strain rate [56, 57], for example, demonstrates

the importance of hydrogen transport in tensile testing. Deformation occurs more or less uniformly in the gauge section in the initial stages of a tensile test (assuming no surface cracking), while diffusion distances are comparatively short (equation 2). Therefore, the fraction of deforming material that is affected by hydrogen is relatively small for typical tensile tests and will depend on the strain rate.

In precracked specimens, on the other hand, damage is localized ahead of the crack tip where stresses and strains are highest. Indeed, Gangloff showed that the critical distance for diffusion ahead of a crack tip is less than ten nanometers for FCC steels [58]; i.e., several orders of magnitude less then the micrometer predicted for diffusion on time scales associated with testing. Therefore, hydrogen diffusion is sufficient to interact with the fracture process ahead of a crack tip and it can be hypothesized that precracked specimens will be relatively insensitive to conventional testing rates, unlike smooth-bar tensile testing.

Testing results for the alloy A-286 (precipitation-strengthening austenitic stainless steel) amplify the differences between testing smooth and precracked specimens. Slow strain-rate tensile tests on A-286 in gaseous hydrogen show no effect of hydrogen [59] (although, more generally, effects of hydrogen are observed in tensile tests of austenitic stainless steels in gaseous hydrogen [60-66]). Indeed, ASTM G142 lists A-286 as the control material for high resistance to hydrogen embrittlement. In contrast, tests with precracked specimens (constant-displacement subcritical crack growth tests [67, 68] and fatigue tests [69]) show a significant effect of gaseous hydrogen on resistance to crack growth for A-286. These results for A-286 substantiate reports of internal hydrogen reducing fracture resistance [70] and show that lack of an observed effect in tensile testing is insufficient to demonstrate that hydrogen does not reduce resistance to cracking.

3.7.4.2 Internal hydrogen

Internal hydrogen can be introduced in metals prior to mechanical testing by several methods, often referred to as hydrogen precharging. The aim of hydrogen precharging is to simulate long-term exposure to hydrogen environments in relatively short-term tests without the complexity of testing in gaseous hydrogen environments (especially at high pressure). At room temperature (and lower), the diffusivity of hydrogen in austenitic stainless steels is sufficiently slow that internal hydrogen is not lost from bulk specimens on time scales of many hours. Although the general consensus is that the hydrogen-deformation interactions are essentially the same for testing in external hydrogen and with internal hydrogen [5, 54, 55], the manifestation of the effects of hydrogen may differ [66] due to differences in boundary conditions (e.g., hydrogen content and distribution) [5, 54, 55].

Electrochemical precharging can produce extremely high hydrogen fugacity (i.e., effective pressure) near the surface, which result in surface cracking and phase transformations [71, 72]. In principle, electrochemical methods can be designed to control hydrogen fugacity to levels consistent with gaseous hydrogen exposure, however, appropriate procedures for austenitic stainless steels have not been demonstrated in the literature. The electrochemistry within cracks, moreover, is generally difficult to evaluate, which is an additional challenge for quantifying hydrogen fugacity in precracked specimens. For these reasons, results from electrochemically precharged materials should be considered with caution in the context of hydrogen-assisted fracture in gaseous hydrogen.

Thermal precharging from gaseous hydrogen is a process of exposing materials to high-pressure gaseous hydrogen at temperatures typically in the range of 200 to 350˚C. The elevated temperature increases the rate of diffusion and the solubility of hydrogen in austenitic stainless

steels without significantly affecting the microstructure. Due to the high diffusivity at elevated temperature, thermal precharging can produce uniform distribution of hydrogen throughout a specimen on time scales of days (unlike electrochemical methods), which has the advantage that hydrogen contents can be quantified. Moreover, hydrogen concentrations that are indicative of gaseous hydrogen service can be produced by thermal precharging [66]. Significant gradients in hydrogen concentration, however, can be difficult to predict due to the influence of surface kinetics.

The distribution of hydrogen within the metal due to hydrogen precharging is generally different compared to testing in gaseous hydrogen [5, 54, 55]. Recent comparisons of tensile tests in gaseous hydrogen and with internal hydrogen, however, show that tensile testing in gaseous hydrogen produces similar reduction of tensile ductility than testing materials with internal hydrogen (Figure 2) [61, 65, 66]. Observed differences between external and internal hydrogen can be related to differences in the evolution of damage as a consequence of hydrogen distribution [66]. Surface cracking, for example, is induced during tensile testing in external hydrogen, while damage is more uniformly distributed with internal hydrogen [66]. Similarity between testing in gaseous hydrogen [73] and with internal hydrogen [74] is also observed for precracked specimens of the stable 21Cr-6Ni-9Mn alloy. Additional testing, as well as simulations that couple the mechanics and hydrogen transport, is needed to better define the test geometries and test conditions for which internal hydrogen is representative of external hydrogen.

3.7.5 Models and mechanisms

3.7.5.1 Models of hydrogen-assisted deformation and fracture

There are numerous models for hydrogen-assisted fracture, which are comprehensively summarized by Lynch [75]. In austenitic stainless steels, decohesion is generally not observed and little evidence exists for the hydrogen-enhanced decohesion (HEDE) model in this class of material. Models based on the embrittlement of hydride phases also are unlikely for austenitic stainless steels, since hydride phases are observed primarily in exceptional cases [76, 77]. The embrittlement of strain-induced martensite is also commonly evoked for the metastable austenitic stainless steels [12, 60-62, 69, 78-81], although direct evidence for this is generally lacking in the literature. Two models have received the most attention, both theoretically and experimentally: adsorption-induced dislocation emission (AIDE) [75, 82, 83] and hydrogen-enhanced localized plasticity (HELP) [84-92]. Both of these models evoke enhanced localized deformation [75], the primary difference being the source of this deformation. The AIDE model is based on hydrogen-surface interactions, while the HELP model is based on hydrogen-dislocation interactions in the bulk.

It is generally conceded that a single mechanism of hydrogen-assisted fracture is unlikely as there are competing processes that predominate for different conditions [75, 86]. Nevertheless, there is strong experimental evidence to support hydrogen-dislocation interactions in austenitic stainless steels [84, 85, 88, 93, 94], including recent studies of deformation in hydrogen-precharged metastable [95] and stable [96] alloys. There is also a strong theoretical framework for understanding hydrogen-dislocation interactions [87, 89-92, 97]; a comprehensive overview

of hydrogen-dislocation interactions is provided in the chapter by Delafosse in this volume. Since hydrogen-dislocation interactions can be used to broadly rationalize observed fracture morphologies, a few of their characteristics are briefly outlined below.

Finite element modeling and *ab initio* calculations show similar features of hydrogen-dislocation interactions [87, 89-92, 97]. The primary effects of hydrogen are to (1) stabilize edge dislocations and (2) elastically shield stress centers associated with dislocations. Experimental observations using *in situ* transmission electron microscopy (TEM) [88, 98] confirm the theoretical finding that hydrogen stabilizes edge dislocations and promotes planar deformation. Only screw dislocations are capable of cross slip, an important mechanism for relaxing stress at dislocation pile-ups and homogenizing deformation. Additionally, hydrogen atmospheres associated with dislocations elastically shield the dislocations from stress centers such as other dislocations [87, 91, 99] as well as reducing the Peierls stress [89]. These characteristics of hydrogen enhance dislocation mobility in the metal and contribute to deformation instabilities [100]. Additionally, the influence of hydrogen in screening stress increases the density of dislocations in pile-ups, which increases stress concentrations at the microstructural obstacles that create these pile-ups [92].

3.7.5.2 Strain-induced martensite

The role of martensite in hydrogen-assisted fracture of austenitic stainless steels deserves special comment. Degradation of ductility in austenitic stainless steels in hydrogen environments is often attributed or correlated to the formation of α'-martensite [12, 60-62, 69, 78-81], particularly when the fracture surfaces are difficult to interpret. Evidence for hydrogen-assisted fracture being induced by α'-martensite is circumstantial and has never been clearly

demonstrated for tests with hydrogen. Remarkably, much of the assertion about the role of martensite is based on comparison between metastable AISI type 304 (or 316) and the lack of effects of gaseous hydrogen on stable AISI type 310 austenitic stainless steel. Stable alloys that show significant effects of gaseous hydrogen (such as 21Cr-6Ni-9Mn [73, 101]) have generally not been considered in studies that focus on martensite as the primary mechanism of hydrogen-assisted fracture. It should not be overlooked that hydrogen has a similar effect on deformation and fracture in both metastable and stable alloys [95, 96, 102], suggesting a common mechanism that cannot be related to α'-martensite.

A variety of studies have attempted to address the role of strain-induced martensite in hydrogen-assisted fracture of austenitic stainless steels. X-ray diffraction and *in situ* TEM studies addressed this issue based on definitive measurements of the interactions between fracture and martensite; these studies have shown that martensite participates in fracture (as it must being present in the microstructure) but they have failed to show that martensite dominates or controls fracture [103, 104]. Several studies have also shown that pre-existing martensite does not reduce tensile ductility of AISI type 304 alloys when exposed to hydrogen [105, 106]; it was hypothesized that the effects of hydrogen are related to the dislocation structure [105], or more precisely to hydrogen-deformation interactions. In short, α'-martensite is neither necessary nor sufficient to explain hydrogen-assisted fracture of austenitic stainless steels [78, 107-109].

Recent work suggests that ε-martensite can be promoted in austenitic stainless steels when deformed in the presence of hydrogen. In thermally-precharged AISI type 304 [95] and stable 21Cr-6Ni-9Mn [96], ε-martensite is promoted at the expense of deformation twinning, while less ε-martensite was observed in an alloy with higher nickel content. While the implications of these

observations are not yet clear, they highlight the importance of SFE on deformation in the presence of hydrogen [96] and show that the role of martensite in hydrogen-assisted fracture is incompletely understood.

3.7.6 Observations of hydrogen-assisted fracture

The characteristics of fracture in hydrogen environments are quite diverse, reflecting the large variation in resistance of austenitic stainless steels to hydrogen-assisted fracture. The observed fracture modes in austenitic stainless steels can be idealized in three broad categories: (1) microvoid coalescence (MVC); (2) interface fracture (including intergranular fracture); and (3) cleavage (although hydrogen-induced cleavage is not typically observed in austenite). In many cases more than one fracture mode is apparent on a given fracture surface [74, 102], suggesting either a common origin of the damage or competing mechanisms. Other fracture modes can be represented by these categories or combination thereof; in the case of slip band fracture, for example, voids nucleate at slip band intersections (MVC), followed by growth along the slip band (interface fracture) [110-112].

Microvoid coalescence (MVC) is the classic fracture mode observed for ductile metals, including austenitic stainless steels, which feature equiaxed dimples. In hydrogen environments, size and uniformity of the dimples is often changed, exhibiting a spectrum of dimple morphologies from equiaxed (Figure 3) to elongated (Figure 4). Hydrogen can activate additional void nucleation sites, reducing dimple size [113, 114]. Modeling suggestions that hydrogen can also affect void growth by localizing deformation between voids or other damage sites [115]. In other cases, elongated dimples are observed in the presence of hydrogen (Figure 4) in materials that normally

feature equiaxed dimples. This morphology is attributed to voids nucleating at the intersection of deformation bands [8, 74, 102]. Elongated dimples are also observed in alloy systems that deform non-uniformly due to limited number of available slip systems (such as titanium in the absence of hydrogen) [116, 117]. When slip systems are limited, (planar) deformation bands are promoted and the intersection of these bands are local sites of strain accumulation. In this instance, deformation tends to be planar, have regular spacing and intersect along lines, thus voids that nucleate at these intersections appear as parallel, elongated dimples (Figure 4). Promotion of planar deformation in austenitic stainless steels is consistent with hydrogen stabilizing edge dislocations and limiting cross slip. In general, greater variation from equiaxed dimples reflects greater susceptibility to hydrogen-assisted fracture.

Fracture mode changes due to hydrogen can be much more substantial than modifications of dimple morphology. Hydrogen can induce fracture along a variety of interfaces, typically reflecting greater susceptibility to hydrogen-assisted fracture than when MVC is predominant. Intergranular fracture is seldom observed for austenitic stainless steels [118], except in instances where the grain boundaries are decorated with second phases due to sensitization in metastable and stable alloys [12, 61], due to overaging of precipitation strengthened alloys [70, 119], or under particularly extreme environments [112]. Fracture may occur along deformation bands, as in slip band fracture [110-112], or along phase boundaries [105, 120-122]. The presence of second phases, however, does not imply hydrogen-assisted fracture along those boundaries; for example, hydrogen-assisted fracture does not necessarily occur along martensite-austenite boundaries [105] or ferrite-austenite boundaries [123, 124].

Large, flat, facet-like features apparent on the fracture surface of austenitic stainless steels (Figure 5) are attributed to fracture along thermal twin boundaries [95, 102, 125]; this fracture

mode is arguably similar to slip band fracture [110-112]. In type 304 and type 316 alloys, fracture of thermal twin boundaries is generally not observed at room temperature in the presence of hydrogen; however, at subambient temperature, fracture of these boundaries can dominate the appearance of the fracture surface (Figure 5), although only for alloys with low nickel content [102], including stable alloys. Low nickel and low temperature are known to produce more localized deformation in type 304 and type 316 alloys [15], suggesting a link between the intrinsic character of deformation for a given composition and the effects of hydrogen on deformation. Twin boundary fracture is not unique to hydrogen: high-nitrogen and low-nickel austenitic alloys show remarkably similar fracture surfaces in the absence of hydrogen at low temperature. Twin boundary fracture in these alloys is attributed to localized deformation induced by low temperature and short-range ordering [126-128]. In addition, modeling by Chateau et al. have shown that stress on complementary slip planes at the head of dislocation pile-ups is amplified by hydrogen [92]. The complimentary slip plane is precisely the twin boundary. Therefore, twin boundary fracture can be rationalized by the effects of hydrogen on enforcing planar deformation and increasing stress on the twin boundary.

Cleavage fracture is generally not associated with austenite in the context of gaseous hydrogen. However, cleavage fracture (Figure 6) may be an important mode in two-phase microstructures and at inclusions. Although fracture along cleavage planes has not been confirmed in these cases, relatively flat fracture facets are observed across entire ferrite grains in duplex alloys [102, 124] and in welds [122]. In a duplex alloy, it was determined that ferrite fractures, followed by MVC along highly inclined planes in the austenite [124]. Consequently, cracking in the ferrite was attributed to local stress concentrations as a result of enhanced planar deformation in the austenite, which may be a requirement for this form of cleavage fracture in ferrite-austenite

microstructures [122]. Similar observations and conclusions have been drawn for residual ferrite in nominally single-phase austenitic [74, 102].

3.7.7 Trends in hydrogen-assisted fracture

3.7.7.1 Tensile testing

Tensile testing is a simple, effective testing method for establishing many basic trends. Not all characteristics of structural integrity, however, are sensitive to tensile testing as noted in section 3.7.4.1. The effect of strength on fracture resistance is another characteristic that tensile testing does not capture: as shown in Figure 1, the reduction of area of annealed (open symbols) and strain-hardened (closed-symbols) type 316 alloys is similar when hydrogen-precharged [129, 130]. In fracture mechanics tests, on the other hand, strength is expected to significantly affect the fracture resistance (with or without hydrogen). The effects of pressure are also not always clearly evident in tensile tests: only modest differences in reduction of area were noted in tests performed in gaseous hydrogen at pressure of 1 MPa and 40 MPa [66] and for tests between 15 and 70 MPa [6]. On the other hand, tensile testing is particularly effective at providing insight on parameters that affect deformation in austenitic stainless steels, such as composition and temperature.

<u>Composition</u>

In general, compositional effects on hydrogen-assisted fracture in austenitic stainless steels is dominated by nickel content [6, 7, 62] and, to some extent, nitrogen [131, 132]. Other alloying constituents have not been studied comprehensively, although there is little evidence to suggest a direct primary role. Differences in chromium and molybdenum, for example, might explain some

of the scatter in Figure 2, although a single trend with nickel describes the data for both type 304 and type 316 alloys. Impurity elements (including processing elements such as Mn and Si) also do not seem to have a significant effect on hydrogen-assisted fracture of austenitic stainless steels [6, 7, 133].

Nickel content is clearly a dominant characteristic for resistance to hydrogen-assisted fracture in austenitic stainless steels [7, 41, 62, 66, 118, 129, 131, 133]. Caskey [6, 7] presents a striking plot of relative tensile ductility as a function of nickel content for Fe-Cr-Ni alloys in the presence of hydrogen, showing a precipitous drop in tensile ductility for alloys with 10 wt% nickel or less. More recent tensile data show a gradual increase in reduction of area as a function of increasing nickel content (above 10 wt%) for a variety of metastable and stable austenitic stainless steels (Figure 1). Stable alloys, such as 21Cr-6Ni-9Mn, are susceptible to hydrogen-assisted fracture and show similar fracture morphologies to the metastable alloys, suggesting that the role of nickel is more complicated than its role on austenite stability, as attributed in the literature [62, 131, 132]. Rather the importance of nickel is better correlated with its effect on deformation: low nickel content tends to promote the localization of plasticity into planar deformation structures [15], a feature that exacerbates hydrogen-assisted fracture [74, 85, 102].

A broad range of commercial alloys based on type 304 and type 316 was tested in Refs. [63, 64, 66, 129, 134], and these studies show no influence of carbon on susceptibility to hydrogen-assisted fracture. In contrast, some reports in the literature imply that low carbon content is important for resistance to hydrogen-assisted fracture [60, 81]. These latter results can be explained by differences in nickel content (Figure 1). Sensitization, on the other hand, may promote susceptibility to hydrogen. Carbides are believed to have little, if any, direct effect on hydrogen-assisted fracture of austenitic stainless steels [12, 108, 135]; however, carbide

precipitation is essentially a form of macrosegregation, which enhances hydrogen-assisted fracture [12].

Nitrogen affects deformation in austenitic stainless steels [16], thus nitrogen can be expected to play a role in tensile properties in the presence of hydrogen [118, 131]. The trends with nitrogen, however, are not yet clear and require further study. The tensile ductility of stable 21Cr-6Ni-9Mn alloys is lower for heats with higher nitrogen content (for the approximate range of 0.2 to 0.5 wt% nitrogen); in addition, the fracture mode changes from MVC at low nitrogen content to intergranular fracture at high nitrogen content [118]. These observations are attributed to the effect of nitrogen on lowering SFE and enhancing planar deformation [25]. In laboratory heats of Fe-Cr-Ni alloys based on AISI type 316, on the other hand, the tensile ductility in gaseous hydrogen is greater with higher nitrogen [131, 132]. In this case, the improved ductility with higher nitrogen is attributed to the enhanced stability of the austenite [131, 132]. Nitrogen at low concentrations is reported to have little effect on SFE in austenitic stainless steels [24], while others suggest nitrogen enhances planar slip [16], therefore the results above cannot be easily explained by an effect of nitrogen on deformation. On the other hand, it has also been hypothesized that nitrogen may promote short-range ordering (SRO), which would enhance localized deformation [25, 85]. In summary, although the trends with nitrogen appear contradictory, nitrogen can enhance planar slip (under some conditions at least) and this characteristic generally correlates with greater susceptibility to hydrogen.

The impact of composition can be very localized, as exemplified by comparison of different product forms of nearly identical type 316L. Testing of compositionally similar bar and plate resulted in measurable differences in macrosegregation and reduction of area in gaseous hydrogen [136]. Similarly, characterization of fracture surfaces from a type 316 alloy revealed

lower nickel content locally at features that reflect greater susceptibility to hydrogen [102]. The effects of macrosegregation are difficult to generalize because these effects will depend on the magnitude of the segregation as well as the distribution of the segregation (e.g., segregation in planes versus stringers [136]). Nevertheless, these results suggest that appropriately homogenized wrought alloys will likely have superior resistance to hydrogen-assisted fracture compared to similar alloys that display macrosegregation. Although experimental data is lacking, these observations can be extended to other microstructures that can be characterized by significant macrosegregation, such as welds and cast alloys. In general, macrosegregation is likely to produce greater susceptibility to the effects of hydrogen than bulk composition might suggest.

Temperature

As temperature is lowered the effect of hydrogen on tensile ductility is greater. Most reports find that tensile ductility displays a minimum at temperature near 200 K for both tests in gaseous hydrogen [62, 137] and hydrogen-precharged materials [6, 7, 133]. Tensile ductility increases with further reduction of temperature to values comparable to those found in tests without hydrogen. Increased ductility at temperatures lower than 200 K is commonly attributed to limited hydrogen diffusion at very low temperature [62]. This interpretation suggests that this minimum is governed by strain rate; given additional time for hydrogen diffusion during the test (i.e, slower testing rates), tensile ductility could continue to decrease. Other interpretations relate this minimum to the transport of hydrogen atmospheres with moving dislocations, which becomes increasing difficult at low temperature [87, 138]. Slow strain rate tensile tests in liquid hydrogen and cold helium (both nominally at 20 K), on the other hand, show significantly greater loss of reduction of area in gaseous hydrogen [139]. The implication of this last result needs further

clarification, but it seems to suggest that the temperature minimum near 200 K may represent a local minimum.

3.7.7.2 Fracture resistance testing

In the context of gaseous hydrogen environments, there is a paucity of studies in the literature that assess fracture resistance of austenitic stainless steels using fracture mechanics methodologies. The influence of temperature and composition on fracture resistance in gaseous hydrogen, for example, has not been studied. The data in Figure 7 show that strength differences are more important for fracture resistance than for tensile properties. There is an overall trend of lower fracture resistance as strength is increased, as generally expected for metals with similar microstructures in the absence of hydrogen.

Fracture testing also amplifies other microstructural considerations. In the 22Cr-13Ni-5Mn alloy, fracture resistance was found to be governed by the orientation of platelets of second phase inclusions with a secondary influence of hydrogen [140]. While the reduction of fracture resistance due to hydrogen for the two orientations was similar, the absolute fracture resistance with internal hydrogen is a reflection of the effect of inclusion orientation on fracture and not a dominant effect of hydrogen (as denoted by the difference between closed squares at nominally the same strength in Figure 7; the same effect is observed at two strength levels).

The data in Figure 7 also show that the fracture resistance of precipitation-strengthened A-286 is not significantly greater (and arguably less) than the fracture resistance of strain-hardened stable and metastable alloys with comparable strength. Tensile testing of A-286 led to the common interpretation that A-286 is “negligibly embrittled” by gaseous hydrogen [57, 59, 141], however,

for resistance to crack propagation in hydrogen, A-286 is similar to other austenitic stainless steels (Figure 7), as well as quench and tempered steels with similar strength [142, 143].

3.7.7.3 Fatigue testing

Evaluating fatigue properties of austenitic stainless steels is an area of active research [69, 130, 144-150]. Of the more conventional test methodologies that are used to study effects of hydrogen on fatigue, fatigue-life tests show essentially no effect of gaseous hydrogen on annealed and strain-hardened type 316L [130, 144]. An apparent increase in fatigue-life was reported for rotating beam fatigue testing of two hydrogen-precharged type 316 alloys (strain-hardened) [148]; however, when the stress amplitude is normalized by strength (internal hydrogen can increase strength by 15% or more [66, 129, 151]), the fatigue life is unchanged by hydrogen. Fatigue crack growth rates of type 316 alloys are also unaffected in external hydrogen [130, 144] and with internal hydrogen [150]. These tests were performed primarily at frequency of 1 Hz (or greater) and with alloys of nominally 11 to 12 wt% nickel content. Additionally, the specimen geometries are conventional smooth cylindrical specimens (fatigue life) and compact tension specimens (fatigue crack growth).

Innovative test methods reveal greater effects of hydrogen on fatigue of austenitic stainless steels than those described above. One method uses axially notched tubes that are internally pressurized with gaseous hydrogen and load cycled by pressurizing externally with water [69]. These fatigue tests show no effect of frequency in the range of 0.01 to 0.05 Hz for high-nickel type 316L, commensurate with the results from conventional cylindrical specimens. For type 304 (with comparatively less nickel), however, the cycles to failure is reduced for tests with hydrogen exposure at frequency of 0.002 Hz compared to tests at higher frequency [69]. These authors of this work interpret the higher sensitivity of type 304 compared to type 316L to greater propensity

to form strain-induced martensite [69]. The authors also report a greater reduction in fatigue life for A-286 [69], which does not form martensite .

The hole-drilled axial fatigue specimen is another geometry that has been extensively exploited in recent fatigue studies using internal hydrogen [145-147, 149]. This geometry is employed to simulate short crack behavior; however, the conventional framework for applying fracture mechanics to fatigue crack growth is not applicable and an alternative framework to generalize short crack behavior is less well developed [152]. In general, the results from these studies are consistent with those described above: lower nickel alloys (from the type 304 and type 316 families) are more affected by hydrogen and lower frequency enhances the effects of hydrogen. More study, however, is necessary to place this work into the context of other fatigue studies; in particular, the role of hydrogen-strengthening on crack initiation and propagation in materials with internal hydrogen.

The available fatigue data for austenitic stainless steels is relatively scarce. Superficially, nickel appears to be an important materials characteristic for hydrogen-assisted fatigue. It has been suggested that this is related to strain-induced martensite acting as a pathway for hydrogen distribution in metastable alloys [145-147], the implication being that lower frequency is needed to induce hydrogen-assisted fatigue in comparatively stable alloys. Hydrogen-enhanced localized deformation is also used to explain the observed behaviors in fatigue [149], suggesting alternative interpretations for the role of nickel. Fundamental experimental and modeling studies are still needed to more generally illuminate the relationship between hydrogen transport and hydrogen-deformation interactions during fatigue in these alloys and to elucidate the materials and environmental conditions (strength, composition, temperature, etc.) that significantly affect fatigue resistance.

3.7.8 Summary and future directions

Nickel and temperature are two critically important parameters for assessing tensile ductility in the presence of hydrogen. The established trends can be understood in the framework of localized deformation: parameters that enhance localized deformation (such as low temperature and low nickel content) promote the effects of hydrogen. Other microstructural characteristics that promote localized deformation appear to have similar effects, such as ordering and coherent precipitation.

Mechanistically, it is generally accepted that hydrogen also promotes localized deformation. Although there is some disagreement on the general importance of hydrogen-enhanced localized plasticity, the theoretical framework of hydrogen-dislocation interactions provides a robust platform for interpreting observed fracture modes in austenitic stainless steels. While this framework is well developed (Delafosse, this volume), comprehensive experimental validation for austenitic stainless steels remains. Additional study is also required to formalize the link between the effects of hydrogen on deformation and the hypothesized fracture processes. In contrast, there is little direct experimental or theoretical evidence supporting a mechanistic role for martensite in hydrogen-assisted fracture. The similarity between hydrogen-assisted fracture in stable and metastable alloys suggests a secondary role for strain-induced martensite, although this role of martensite is incompletely understood and cannot be discounted.

In general, accepted trends for hydrogen-assisted fracture in austenitic stainless steels are based on the large number of tensile studies. In contrast, the available data from fracture testing and fatigue testing is relatively scarce. Additional testing is necessary to assess the tensile trends

under conditions of crack growth. Models that combine crack-tip mechanics and hydrogen transport are also needed to guide fundamental tests designed to illuminate the details of the fracture process. Crack initiation in gaseous hydrogen has not been discussed in this chapter, primarily because it is an area that as not been received critical attention for the austenitic stainless steels; however, crack initiation and the behavior of short cracks are areas of interest both to hydrogen-assisted fracture and more broadly in the fracture community.

Acknowledgments

Sandia is a multiprogram laboratory operated by Sandia Corporation, a wholly owned subsidiary of Lockheed Martin Corporation, for the U.S. Department of Energy's National Nuclear Security Administration under contract DE-AC04-94AL85000.

References

1. R.P. Gangloff, Hydrogen assisted fracture of high strength alloys, in: Milne I, Ritchie RO and Karihaloo B, editors, Comprehensive Structural Integrity, volume 6, Elsevier Science, New York NY, 2003, pp. 31-101.
2. ASME, Hydrogen Standardization Interim Report for Tanks, Piping, and Pipelines (STP/PT-003), American Society of Mechanical Engineers (ASME), New York, 2005.
3. H.E. Hanninen, Influence of metallurgical variables on environment-sensitive cracking of austenitic alloys, Inernational Metals Reviews 24 (1979) 85-135.
4. A.W. Thompson and I.M. Bernstein, The Role of Metallurgical Variables in Hydrogen-Assisted Environmental Fracture, in: Fontana MG and Staehle RW, editors, Advances in Corrosion Science and Technology, volume 7, Plenum Publishing Corporation, New York, 1980, pp. 53-175.
5. H.G. Nelson, Hydrogen Embrittlement, in: Briant CL and Banerji SK, editors, Embrittlement of Engineering Alloys, Treatise on Materials Science and Technology, volume 25, Academic Press, New York, 1983, pp. 275-359.

6. G.R. Caskey, Hydrogen Compatibility Handbook for Stainless Steels (DP-1643), DP-1643, EI du Pont Nemours, Savannah River Laboratory, Aiken SC, June 1983.
7. G.R. Caskey, Hydrogen Effects in Stainless Steels, in: Oriani RA, Hirth JP and Smialowski M, editors, Hydrogen Degradation of Ferrous Alloys, Noyes Publications, Park Ridge NJ, 1985, pp. 822-862.
8. N.R. Moody, S.L. Robinson and W.M. Garrison, Hydrogen effects on the properties and fracture modes of iron-based alloys, Res Mechanica 30 (1990) 143-206.
9. R.A. Lula, Stainless Steel (revised from "An Introduction to Stainless Steel" by JG Parr and A Hanson), American Society for Metals, Metals Park OH, 1986.
10. A.W. Thompson and J.A. Brooks, Hydrogen Performance of Precipitation-Strengthened Stainless Steels Based on A-286, Metall Trans 6A (1975) 1431-1442.
11. K.H. Lo, C.H. Shek and J.K.L. Lai, Recent developments in stainless steels, Materials Science and Engineering R 65 (2009) 39-104.
12. G. Han, J. He, S. Fukuyama and K. Yokogawa, Effect of strain-induced martensite on hydrogen environment embrittlement of sensitized austenitic stainless steels at low temperatures, Acta Mater 46 (1998) 4559-4570.
13. D. Peckner and I.M. Bernstein. Handbook of Stainless Steels. New York: McGraw-Hill, 1977.
14. K. Spencer, J.D. Embury, K.T. Conlon, M. Veron and Y. Brechet, Strengthening via the formation of strain-induced martensite in stainless steels, Mater Sci Eng A378-379 (2004) 873-881.
15. J. Talonen and H. Hanninen, Formation of shear bands and strain-induced martensite during plastic deformation of metastable austenitic stainless steels, Acta Mater 55 (2007) 6108-6118.
16. P. Muellner, C. Solenthaler, P. Uggowitzer and M.O. Speidel, On the effect of nitrogen on the dislocation structure of austenitic stainless steel, Mater Sci Eng A164 (1993) 164-169.
17. T.S. Byun, N. Hashimoto and K. Farrell, Deformation mode map of irradiated 316 stainless steel in true stress-dose space, J Nucl Mater 351 (2006) 303-315.
18. T.S. Byun, N. Hashimoto and K. Farrell, Temperature dependence of strain hardening and plastic instability behaviors in austenitic stainless steel, Acta Mater 52 (2004) 3889-3899.
19. L. Vitos, J.-O. Nilsson and B. Johansson, Alloying effect on the stacking fault energy in austenitic stainless steels from first-principles theory, Acta Mater 54 (2006) 3821-3826.
20. L. Vitos, P.A. Korzhavyi and B. Johansson, Evidence of large magnetostructural effects in austenitic stainless steels, Physical Review Letters 96 (2006) 1172101-1172104.
21. R.E. Schramm and R.P. Reed, Stacking Fault Energies of Seven Commercial Austenitic Stainless Steels, Metall Trans 6A (1975) 1345-1351.
22. C.G. Rhodes and A.W. Thompson, The Composition Dependence of Stacking Fault Energy in Austenitic Stainless Steels, Metall Trans 8A (1977) 1901-1905.
23. P.J. Brofman and G.S. Ansell, On the effect of carbon on the stacking fault energy of austenitic stainless steels, Metall Trans 9A (1978) 879-880.
24. R.P. Reed and M.W. Austin, Effect of nitrogen and carbon on FCC-HCP stability in austenitic steels, Scr Metall 23 (1989) 1359-1362.
25. R.E. Stoltz and J.B. VanderSande, The Effect of Nitrogen on Stacking Fault Energy of Fe-Ni-Cr-Mn Steels, Metall Trans 11A (1980) 1033-1037.

26. C. San Marchi, B.P. Somerday and S.L. Robinson, Permeability, Solubility and Diffusivity of Hydrogen Isotopes in Stainless Steels at High Gas Pressure, Int J Hydrogen Energy 32 (2007) 100-116.
27. W.G. Perkins, Permeation and Outgassing of Vacuum Materials, J Vac Sci Technol 10 (1973) 543-556.
28. J.P. Hirth, Effects of hydrogen on the properties of iron and steel, Metall Trans 11A (1980) 861-890.
29. R.A. Oriani, The Physical and Metallurgical Aspects of Hydrogen in Metals, Fusion Technology 26 (1994) 235-66.
30. C. San Marchi and B.P. Somerday, Thermodynamics of Gaseous Hydrogen and Hydrogen Transport in Metals (1098-HH08-01), in: Mater Res Soc Symp Proc Vol 1098 (MRS 2008 Spring Meeting, San Francisco CA, 2008), Materials Research Society,
31. G.J. Thomas, Hydrogen trapping in FCC metals, in: Bernstein IM and Thompson AW, editors, Hydrogen Effects in Metals, Proceedings of the Third International Conference on Effect of Hydrogen on Behavior of Materials (Moran WY, 1980), The Metallurgical Society of AIME, New York, 1981, pp. 77-85.
32. H.A. Wriedt and R.A. Oriani, Effect of tensile and compressive elastic stress on equilibrium hydrogen solubility in a solid, Acta Metall 18 (1970) 753-760.
33. H.P. van Leeuwen, The kinetics of hydrogen embrittlement: a quantitative diffusion model, Eng Fract Mech 6 (1974) 141-161.
34. M.R. Louthan and R.G. Derrick, Hydrogen Transport in Austenitic Stainless Steel, Corros Sci 15 (1975) 565-577.
35. T.-P. Perng and C.J. Altstetter, Effects of Deformation on Hydrogen Permeation in Austenitic Stainless Steels, Acta Metall 34 (1986) 1771-1781.
36. X.K. Sun, J. Xu and Y.Y. Li, Hydrogen Permeation Behaviour in Austenitic Stainless Steels, Mater Sci Eng A114 (1989) 179-187.
37. A.D. LeClaire, Permeation of Gases Through Solids: 2. An assessment of measurements of the steady-state permeability of H and its isotopes through Fe, Fe-based alloys, and some commercial steels, Diffusion and Defect Data 34 (1983) 1-35.
38. X.K. Sun, J. Xu and Y.Y. Li, Hydrogen permeation behavior in metastable austenitic stainless steels 321 and 304, Acta Metall 37 (1989) 2171-2176.
39. J. Xu, X.K. Sun, W.X. Chen and Y.Y. Li, Hydrogen Permeation and Diffusion in Iron-base Superalloys, Acta Metall Mater 41 (1993) 1455-1459.
40. J.K. Tien, A.W. Thompson, I.M. Bernstein and R.J. Richards, Hydrogen transport by dislocations, Metall Trans 7A (1976) 821-829.
41. M.R. Louthan, G.R. Caskey, J.A. Donovan and D.E. Rawl, Hydrogen Embrittlement of Metals, Mater Sci Eng 10 (1972) 357-368.
42. J.A. Donovan, Accelerated evolution of hydrogen from metals during plastic deformation, Metall Trans 7A (1976) 1677-1683.
43. J. Chene, M. Aucouturier, R. Arnould-Laurent, P. Tison and J.-P. Fidelle, Hydrogen Transport by Deformation and Hydrogen Embrittlement in Selected Stainless Steels, in: Bernstein IM and Thompson AW, editors, Hydrogen Effects in Metals, Proceedings of the Third International Conference on Effect of Hydrogen on Behavior of Materials (Moran WY, 1980), The Metallurgical Society of AIME, New York, 1981, pp. 583-595.
44. A.M. Brass and J. Chene, Hydrogen uptake in 316L stainless steel: Consequences on the tensile properties, Corros Sci 48 (2006) 3222-3242.

45. B. Ladna and H.K. Birnbaum, A study of hydrogen transport during plastic deformation, Acta Metall 35 (1987) 1775-1778.
46. A. Michels, W. De Graff, T. Wassenaar, J.M.H. Levelt and P. Louwerse, Compressibility Isotherms of Hydrogen and Deuterium at Temperatures between -175˚C and +150˚C (at Densities up to 960 Amagat), Physica 25 (1959) 25-42.
47. N.B. Vargaftik, Tables on the Thermophysical Properties of Liquids and Gases: in Normal and Dissociated States, Hemisphere Publishing Corporation, London, 1975.
48. K.G. McLennan and E.M. Gray, An equation of state for deuterium gas to 1000 bar, Meas Sci Technol 15 (2004) 211-215.
49. M.R. Louthan and R.G. Derrick, Permeability of Nickel to High Pressure Hydrogen Isotopes, Scr Metall 10 (1976) 53-55.
50. N.R. Quick and H.H. Johnson, Permeation and Diffusion of Hydrogen and Deuterium in 310 Stainless Steel, 472K to 779K, Metall Trans 10A (1979) 67-70.
51. W.A. Swansiger and R. Bastasz, Tritium and Deuterium Permeation in Stainless Steels: Influence of Thin Oxide Films, J Nucl Mater 85 & 86 (1979) 335-339.
52. K.S. Forcey, D.K. Ross, J.C.B. Simpson and D.S. Evans, Hydrogen Transport and Solubility in 316L and 1.4914 Steels for Fusion Reactor Applications, J Nucl Mater 160 (1988) 117-124.
53. T. Shiraishi, M. Nishikawa, T. Tamaguchi and K. Kenmotsu, Permeation of multi-component hydrogen isotopes through austenitic stainless steels, J Nucl Mater 273 (1999) 60-65.
54. J.P. Fidelle, Closing Commentary–IHE-HEE: Are They the Same?, in: Hydrogen Embrittlement Testing, ASTM STP 543, American Society for Testing and Materials, Philadelphia PA, 1974, pp. 267-272.
55. H.G. Nelson, Closing Commentary–IHE-HEE: Are They the Same?, in: Hydrogen Embrittlement Testing, ASTM STP 543, American Society for Testing and Materials, Philadelphia PA, 1974, pp. 273-274.
56. J.H. Holbrook and A.J. West, The Effect of Temperature and Strain Rate on the Tensile Properties of Hydrogen Charged 304L, 21-6-9, and JBK 75, in: Bernstein IM and Thompson AW, editors, Hydrogen Effects in Metals, Proceedings of the Third International Conference on Effect of Hydrogen on Behavior of Materials (Moran WY, 1980), The Metallurgical Society of AIME, New York, 1981, pp. 655-663.
57. E.J. Vesely, R.K. Jacobs, M.C. Watwood and W.B. McPherson, Influence of Strain Rate on Tensile Properties in High-Pressure Hydrogen, in: Thompson AW and Moody NR, editors, Hydrogen Effects in Materials, Proceedings of the Fifth International Conference on the Effect of Hydrogen on the Behavior of Materials (Moran WY, 1994), TMS, Warrendale PA, 1996, pp. 363-374.
58. R.P. Gangloff, Diffusion control of hydrogen environment embrittlement in high strength alloys, in: Moody NR, Thompson AW, Ricker RE, Was GW and Jones RH, editors, Hydrogen Effects on Materials Behavior and Corrosion Deformation Interactions, Proceedings of the 2002 International Hydrogen Conference (Moran WY, 2002), TMS, Warrendale PA, 2003, pp. 477-497.
59. R.P. Jewitt, R.J. Walter, W.T. Chandler and R.P. Frohmberg, Hydrogen Environment Embrittlement of Metals, NASA CR-2163, Rocketdyne for the National Aeronautics and Space Administration, Canoga Park CA, March 1973.

60. S. Fukuyama, M. Imade, Z. Lin and K. Yokogawa, Hydrogen embrittlement of metals in 70 MPa hydrogen at room temperature (PVP2005-71628), in: Proceedings of PVP-2005: ASME Pressure Vessels and Piping Division Conference (Denver CO, 2005), July 17-21, 2005,
61. S. Fukuyama, M. Imade and K. Yokogawa, Development of new material testing appartus in high-pressure hydrogen and evaluation of hydrogen gas embrittlement of metals (PVP2007-26820), in: Proceedings of PVP-2007: ASME Pressure Vessels and Piping Division Conference (San Antonio TX, 2007), ASME,July 22-26, 2007,
62. L. Zhang, M. Wen, M. Imade, S. Fukuyama and K. Yokogawa, Effect of nickel equivalent on hydrogen gas embrittlement of austenitic stainless steels based on type 316 at low temperatures, Acta Mater 56 (2008) 3414-3421.
63. T. Michler, A.A. Yukhimchuk and J. Naumann, Hydrogen environment embrittlement testing at low temperatures and high pressures, Corros Sci 60 (2008) 3519-3526.
64. T. Michler and J. Naumann, Hydrogen environment embrittlement of austenitic stainless steels at low temperatures, Int J Hydrogen Energy 33 (2008) 2111-2122.
65. M. Imade, L. Zhang, M. Wen, T. Iijima, S. Fukuyama and K. Yokogawa, Internal reversible hydrogen embrittlement and hydrogen gas embrittlement of austenitic stainless steels based on type 316 (PVP2009-77605), in: 2009 ASME Pressure Vessels and Piping Conference (Prague, Czech Republic, 2009), ASME,
66. C. San Marchi, T. Michler, K.A. Nibur and B.P. Somerday, On the physical differences between tensile testing of type 304 and 316 austenitic stainless steels with internal hydrogen and in external hydrogen, Int J Hydrogen Energy 35 (2010) 9736-9745.
67. M.W. Perra, Sustained-Load Cracking of Austenitic Steels in Gaseous Hydrogen, in: Louthan MR, McNitt RP and Sisson RD, editors, Environmental Degradation of Engineering Materials in Hydrogen, Laboratory for the Study of Environmental Degradation of Engineering Materials, Virginia Polytechnic Institute, Blacksburg VA, 1981, pp. 321-333.
68. M.W. Perra and R.E. Stoltz, Sustained-Load Cracking of a Precipitation-Strengthened Austenitic Steel in High-Pressure Hydrogen, in: Bernstein IM and Thompson AW, editors, Hydrogen Effects in Metals, Proceedings of the Third International Conference on Effect of Hydrogen on Behavior of Materials (Moran WY, 1980), The Metallurgical Society of AIME, New York, 1981, pp. 645-653.
69. T. Omura, M. Miyahara, H. Semba, M. Igarashi and H. Hirata, Evaluation of hydrogen environment embrittlement and fatigue properties of stainless steels in high pressure gaseous hydrogen (investigation of materials properties in high pressure gaseous hydrogen-2) (PVP2007-26496), in: Proceedings of PVP-2007: ASME Pressure Vessels and Piping Division Conference (San Antonio TX, 2007), ASME,22-26 July, 2007,
70. B.C. Odegard, S.L. Robinson and N.R. Moody, Effects of Internal Hydrogen on the Toughness and Fracture of Forged JBK-75 Stainless Steel, in: Thompson AW and Moody NR, editors, Hydrogen Effects in Materials, Proceedings of the Fifth International Conference on the Effect of Hydrogen on the Behavior of Materials (Moran WY, 1994), TMS, Warrendale PA, 1996, pp. 591-598.
71. H. Hanninen, T. Hakkarainen and P. Nenonen, Effect of ageing on embrittlement and microstructures in hydrogen charged then specimens of austenitic stainless steel, in: Bernstein IM and Thompson AW, editors, Hydrogen Effects in Metals, Proceedings of the

Third International Conference on Effect of Hydrogen on Behavior of Materials (Moran WY, 1980), The Metallurgical Society of AIME, New York, 1981, pp. 575-583.
72. D. Eliezer, Hydrogen assisted cracking in type 304L and 316L stainless steel, in: Hydrogen Effects in Metals, Proceedings of the Third International Conference on Effect of Hydrogen on Behavior of Materials (Moran WY, 1980), The Metallurgical Society of AIME, New York, 1981, pp. 565-574.
73. C. San Marchi. 2010.
74. K.A. Nibur, B.P. Somerday, D.K. Balch and C. San Marchi, The role of localized deformation in hydrogen-assisted crack propagation in 21Cr-6Ni-9Mn stainless steel, Acta Mater 57 (2009) 3795-3809.
75. S.P. Lynch, Progress towards understanding mechanisms of hydrogen embrittlement and stress corrosion cracking, in: Corrosion 2007 (Nashville TN, 2007), NACE International,pp. paper no. 07493.
76. N. Narita, C.J. Altstetter and H.K. Birnbaum, Hydrogen-related phase transformations in austenitic stainless steels, Metall Trans 13A (1982) 1355-1365.
77. M. Hoelzel, S.A. Danilkin, H. Ehrenberg, D.M. Toebbens, T.J. Udovic, H. Fuess and H. Wipf, Effects of high-pressure hydrogen charging on the structure of austenitic stainless steels, Mater Sci Eng A384 (2004) 255-261.
78. C.L. Briant, Hydrogen assisted cracking of austenitic stainless steels, in: Bernstein IM and Thompson AW, editors, Hydrogen Effects in Metals, Proceedings of the Third International Conference on Effect of Hydrogen on Behavior of Materials (Moran WY, 1980), The Metallurgical Society of AIME, New York, 1981, pp. 527-541.
79. R.E. Stoltz and A.J. West, Hydrogen Assisted Fracture in FCC Metals and Alloys, in: Bernstein IM and Thompson AW, editors, Hydrogen Effects in Metals, Proceedings of the Third International Conference on Effect of Hydrogen on Behavior of Materials (Moran WY, 1980), The Metallurgical Society of AIME, New York, 1981, pp. 541-553.
80. D. Hardie and J.J.F. Butler, Effect of hydrogen charging on fracture behaviour of 304L stainless steel, Mater Sci Technol 6 (1990) 441-446.
81. S. Fukuyama, M. Imade, T. Iijima and K. Yokogawa, Development of new material testing apparatus in 230 MPa hydrogen and evaluation of hydrogen gas embrittlement of metals (PVP2008-61849), in: Proceedings of PVP-2008: ASME Pressure Vessels and Piping Division Conference (Chicago IL, 2008), ASME,July 27-31, 2008,
82. S.P. Lynch, Environmentally assisted cracking: overview of evidence for an adsorption-induced localised-slip process, Acta Metall 38 (1988) 2639-2661.
83. S.P. Lynch, Metallographic contributions to understanding mechanisms of environmentally assisted cracking, Metallography 23 (1989) 147-171.
84. D.G. Ulmer and C.J. Altstetter, Hydrogen-induced strain localization and failure of austenitic stainless steels at high hydrogen concentrations, Acta Metall Mater 39 (1991) 1237-1248.
85. D.P. Abraham and C.J. Altstetter, Hydrogen-enhanced localization of plasticity in an austenitic stainless steel, Metall Mater Trans 26A (1995) 2859-2871.
86. H.K. Birnbaum, I.M. Robertson, P. Sofronis and D. Teter, Mechanisms of Hydrogen Related Fracture - A Review, in: Magnin T, editor, Corrosion-Deformation Interactions, Proceedings of the Second International Conference on Corrosion-Deformation Interactions, CDI 96 (ECF 21), Woodhead Publishing Limited, Cambridge, 1997, pp. 172-195.

87. H.K. Birnbaum and P. Sofronis, Hydrogen-enhanced localized plasticity–a mechanism for hydrogen-related fracture, Mater Sci Eng A176 (1994) 191-202.
88. I.M. Robertson, The effect of hydrogen on dislocation dynamics, Eng Fract Mech 68 (2001) 671-692.
89. G. Lu, Q. Zhang, N. Kioussis and E. Kaxiras, Hydrogen-enhanced local plasticity in aluminum: an ab initio study, Physical Review Letters 87 (2001) 095501-1 - 095501-4.
90. G. Lu, D. Orlikowski, I. Park, O. Politano and E. Kaxiras, Energetics of hydrogen impurities in aluminum and their effect on mechanical properties, Phys Rev B 65 (2002) 064102.
91. J.P. Chateau, D. Delafosse and T. Magnin, Numerical simulations of hydrogen-dislocation interactions in fcc stainless steels. Part I: hydrogen-dislocation interactions in bulk crystals, Acta Mater 50 (2002) 1507-1522.
92. J.P. Chateau, D. Delafosse and T. Magnin, Numerical simulations of hydrogen-dislocation interactions in fcc stainless steels. Part II: hydrogen effects on crack tip plasticity at a stress corrosion crack, Acta Mater 50 (2002) 1523-1538.
93. C.J. Altstetter and D. Abraham, Model for plasticity-enhanced decohesion fracture, in: Thompson AW and Moody NR, editors, Hydrogen Effects in Materials, Proceedings of the Fifth International Conference on the Effect of Hydrogen on the Behavior of Materials (Moran WY, 1994), TMS, Warrendale PA, 1996, pp. 599-609.
94. K.A. Nibur, D.F. Bahr and B.P. Somerday, Hydrogen effects on dislocation activity in austenitic stainless steel, Acta Mater 54 (2006) 2677-2684.
95. C. San Marchi, N.Y.C. Yang, T.J. Headley and J. Michael, Hydrogen-assisted fracture of low nickel content 304 and 316L austenitic stainless steels, in: 18th European Conference on Fracture (ECF18) (Dresden, Germany, 2010), 30 August - 3 September 2010,
96. C. San Marchi, B.P. Somerday and H.F. Jackson, Hydrogen-assisted deformation and fracture of austenitic stainless steels, in: 2nd International Conference of Engineering Against Fracture (ICEAF II) (Mykonos, Greece, 2011), 22-24 June 2011,
97. P. Sofronis, The influence of mobility of dissolved hydrogen on the elastic response of a metal, J Mech Phys Solids 43 (1995) 1385-1407.
98. P.J. Ferreira, I.M. Robertson and H.K. Birnbaum, Hydrogen effects on the character of dislocations in high-purity aluminum, Acta Mater 47 (1999) 2991-2998.
99. P. Sofronis and H.K. Birnbaum, Mechanics of the hydrogen-dislocation-impurity interactions I. Increasing shear modulus, J Mech Phys Solids 43 (1995) 49-90.
100. Y. Liang, P. Sofronis and N. Aravas, On the effect of hydrogen on plastic instabilities in metals, Acta Mater 51 (2003) 2717-2730.
101. A.J. West and M.R. Louthan, Hydrogen Effects on the Tensile Properties of 21-6-9 Stainless Steel, Metall Trans 13A (1982) 2049-2058.
102. C. San Marchi, K.A. Nibur, D.K. Balch, B.P. Somerday, X. Tang, G.H. Schiroky and T. Michler, Hydrogen-assisted fracture of austenitic stainless steels, in: Somerday BP, Sofronis P and Jones R, editors, Effects of Hydrogen on Materials, Proceedings of the 2008 International Hydrogen Conference (Moran WY, 2008), ASM International, Materials Park OH, 2009, pp. 88-96.
103. A.J. West and J.H. Holbrook, Hydrogen in austenitic stainless steels: effects of phase transformations and stress state, in: Bernstein IM and Thompson AW, editors, Hydrogen Effects in Metals, Proceedings of the Third International Conference on Effect of Hydrogen

on Behavior of Materials (Moran WY, 1980), The Metallurgical Society of AIME, New York, 1981, pp. 607-618.
104. P. Rozenak, I.M. Robertson and H.K. Birnbaum, HVEM studies of the efffects of hydrogen on the deformation and fracture of AISI type 316 austenitic stainless steel, Acta Metall Mater 38 (1990) 2031-2040.
105. J.R. Buckley and D. Hardie, The effect of pre-straining and delta-ferrite on the embrittlement of 304L stainless steel by hydrogen, Corros Sci 34 (1993) 93-107.
106. Y. Mine, K. Tachibana and Z. Horita, Effect of high-pressure torsion processing and annealing on hydrogen embrittlement of type 304 metastable austenitic stainless steel, Metall Mater Trans 41A (2010) 3110-3120.
107. A.W. Thompson, Ductility Losses in Austenitic Stainless Steels Caused by Hydrogen, in: Bernstein IM and Thompson AW, editors, Hydrogen in Metals, Proceedings of the International Conference on the Effects of Hydrogen on Materials Properties and Selection and Structural Design (Champion PA, 1973), American Society of Metals, Metals Park OH, 1974, pp. 91-105.
108. A.W. Thompson, The Behavior of Sensitized 309S Stainless Steel in Hydrogen, Mater Sci Eng 14 (1974) 253-264.
109. J.J. Lewandowski and A.W. Thompson, The effect of austenite stability on sustained load cracking and fracture morphology of stainless steels in 1 atmosphere hydrogen, in: Bernstein IM and Thompson AW, editors, Hydrogen Effects in Metals, Proceedings of the Third International Conference on Effect of Hydrogen on Behavior of Materials (Moran WY, 1980), The Metallurgical Society of AIME, New York, 1981, pp. 629-636.
110. N.R. Moody and F.A. Greulich, Hydrogen-induced slip band fracture in an Fe-Ni-Co superalloy, Scr Metall 19 (1985) 1107-1111.
111. N.R. Moody, R.E. Stoltz and M.W. Perra, Effect of hydrogen on fracture toughness of the Fe-Ni-Co superalloy IN903, Metall Trans 19A (1987) 1469-1482.
112. N.R. Moody, M.W. Perra and S.L. Robinson, Hydrogen pressure and crack tip stress effects on slow crack growth thresholds in an iron-based superalloy, Scr Metall 22 (1988) 1261-1266.
113. A.W. Thompson, Ductile fracture topography: geometrical contributions and effects of hydrogen, Metall Trans 10A (1979) 727-731.
114. D.C. Ahn, P. Sofronis and R.H. Dodds, On hydrogen-induced plastic flow localization during void growth and coalescence, Int J Hydrogen Energy 32 (2007) 3734-3742.
115. B.P. Somerday, D.K. Balch, M. Dadfarnia, K.A. Nibur, C.H. Cadden and P. Sofronis, Hydrogen-assisted crack propagation in austenitic stainless steel fusion welds, Metall Mater Trans 40A (2009) 2350-2362.
116. A. Gysler, G. Luetjering and V. Gerold, Deformation behavior of age-hardened Ti-Mo alloys, Acta Metall 22 (1974) 901-909.
117. R.H. Van Stone, T.B. Cox, J.R. Low and J.A. Psoida, Microstructural aspects of fracture by dimpled rupture, International Metals Review 30 (1985) 157-179.
118. B.C. Odegard, J.A. Brooks and A.J. West, The Effect of Hydrogen on Mechanical Behavior of Nitrogen-Strengthened Stainless Steel, in: Thompson AW and Bernstein IM, editors, Effect of Hydrogen on Behavior of Materials, Proceedings of an International Conference on Effect of Hydrogen on Behavior of Materials (Moran WY, 1975), The Metallurgical Society of AIME, New York, 1976, pp. 116-125.

119. B.C. Odegard and A.J. West, The Effect of eta-phase on the Hydrogen Compatibility of a Modified A-286 Superalloy: Microstructural and Mechanical Properties Observations, in: Bernstein IM and Thompson AW, editors, Hydrogen Effects in Metals, Proceedings of the Third International Conference on Effect of Hydrogen on Behavior of Materials (Moran WY, 1980), The Metallurgical Society of AIME, New York, 1981, pp. 597-606.
120. J.A. Brooks and A.J. West, Hydrogen Induced Ductility Losses in Austenitic Stainless Steel Welds, Metall Trans 12A (1981) 213-223.
121. J.A. Brooks, A.J. West and A.W. Thompson, Effect of Weld Composition and Microstructure on Hydrogen Assisted Fracture of Austenitic Stainless Steels, Metall Trans 14A (1983) 75-84.
122. B.P. Somerday, D.K. Balch, M. Dadfarnia, K.A. Nibur, C.H. Cadden and P. Sofronis, Hydrogen-assisted crack propagation in austenitic stainless steel fusion welds, Metall Mater Trans 40A (2008) 2350-2362.
123. W. Tyson, Embrittlement of Types 316L and 347 weld overlay by post-weld heat treatment and hydrogen, Metall Trans 15A (1984) 1475-1484.
124. C. San Marchi, B.P. Somerday, J. Zelinski, X. Tang and G.H. Schiroky, Mechanical properties of super duplex stainless steel 2507 after gas phase thermal precharging with hydrogen, Metall Mater Trans 38A (2007) 2763-2775.
125. G.R. Caskey, Hydrogen-induced brittle fracture of type 304L austenitic stainless steel, in: Gilbertson LN and Zipp RD, editors, Fractography and Materials Science, ASTM STP733, American Society of Testing and Materials, Philadelphia PA, 1981, pp. 86-77.
126. Y. Tomota, Y. Xia and K. Inoue, Mechanism of low temperature brittle fracture in high nitrogen bearing austenitic steels, Acta Mater 46 (1998) 1577-1587.
127. C. Liu, T. Hashida, H. Takahashi, H. Kuwona and Y. Hamaguchi, A study on fractography in the low-temperature brittle fracture of an 18Cr-18Mn-0.7N austenitic steel, Metall Mater Trans 29A (1998) 791-798.
128. S. Liu, D. Liu and S. Liu, Transgranular fracture in low temperature brittle fracture of high nitrogen austenitic steel, J Mater Sci 42 (2007) 7514-7519.
129. C. San Marchi, B.P. Somerday, X. Tang and G.H. Schiroky, Effects of alloy composition and strain hardening on tensile fracture of hydrogen-precharged type 316 stainless steels, Int J Hydrogen Energy 33 (2007) 889-904.
130. S. Ohmiya and H. Fujii, Mechanical properties of cold worked type 316L stainless steel in high pressure gaseous hydrogen (investigation of materials properties in high pressure gaseous hydrogen-3) (PVP2007-26492), in: Proceedings of PVP-2007: ASME Pressure Vessels and Piping Division Conference (San Antonio TX, 2007), ASME,22-26 July, 2007,
131. L. Zhang, M. Wen, M. Imade, S. Fukuyama and K. Yokogawa, Effect of nickel equivalent on hydrogen environment embrittlement of austenitic stainless steels at low temperatures, in: Gdoutos EE, editor, Fracture of Nano and Engineering Materials and Structures. Proceedings of the 16th European Conference of Fracture (Alexandroupolis, Greece, 2006), Springer,
132. M. Imade, L. Zhang, B. An, T. IIjima, S. Fukuyama and K. Yokogawa, Effect of nitrogen on hydrogen embrittlement of austenitic stainless steels based on type 316LN (PVP2010-25698), in: Proceedings of PVP-2010: ASME Pressure Vessels and Piping Division Conference (Bellevue WA, 2010), American Society of Mechanical Engineers,
133. G.R. Caskey, Hydrogen Damage in Stainless Steel, in: Louthan MR, McNitt RP and Sisson RD, editors, Environmental Degradation of Engineering Materials in Hydrogen, Laboratory

for the Study of Environmental Degradation of Engineering Materials, Virginia Polytechnic Institute, Blacksburg VA, 1981, pp. 283-302.
134. C. San Marchi, B.P. Somerday, X. Tang and G.H. Schiroky, Hydrogen-assisted fracture of type 316 stainless steel at subambient temperature (PVP2008-61240), in: Proceedings of PVP-2008: ASME Pressure Vessels and Piping Division Conference (Chicago IL, 2008), ASME,pp. PVP2008-61240.
135. C.L. Briant, Hydrogen Assisted Cracking of Sensitized 304 Stainless Steel, Metall Trans 9A (1978) 731-733.
136. T. Michler, Y. Lee, R.P. Gangloff and J. Naumann, Influence of macro segregation on hydrogen environment embrittlement of SUS 316L stainless steel, Int J Hydrogen Energy 34 (2009) 3201-3209.
137. D. Sun, G. Han, S. Vaodee, S. Fukuyama and K. Yokogawa, Tensile behaviour of type 304 austenitic stainless steels in hydrogen atmosphere at low temperatures, Mater Sci Technol 17 (2001) 302-308.
138. C. Borchers, T. Michler and A. Pundt, Effect of hydrogen on the mechanical properties of stainless steels, Advanced Engineering Materials 10 (2008) 11-23.
139. P. Deimel and E. Sattler, Austenitic steels of different composition in liquid and gaseous hydrogen, Corros Sci 50 (2008) 1598-1607.
140. K.A. Nibur, B.P. Somerday, C. San Marchi and D.K. Balch, Effects of strength and microstructure on hydrogen-assisted crack propagation in 22Cr-13Ni-5Mn stainless steel forgings, Metall Mater Trans 41A (2010) 3348-3357.
141. R.J. Walter, R.P. Jewitt and W.T. Chandler, On the Mechanism of Hydrogen-Environment Embrittlement of Iron- and Nickel-base Alloys, Mater Sci Eng 5 (1970) 99-110.
142. A.W. Loginow and E.H. Phelps, Steels for Seamless Hydrogen Pressure Vessels, Corrosion 31 (1975) 404-12.
143. K.A. Nibur, C. San Marchi and B.P. Somerday, Fracture and fatigue tolerant steel pressure vessels for gaseous hydrogen (PVP2010-25827), in: Proceedings of PVP-2010: ASME Pressure Vessels and Piping Division Conference (Bellevue WA, 2010), ASME,
144. S. Ohmiya and H. Fujii, Fatigue properties of liner materials used for 35 MPa-class on-board hydrogen fuel tanks, in: Proceedings of PVP-2005: ASME Pressure Vessels and Piping Division Conference (Denver CO, 2005), ASME,17-21 July 2005,
145. Y. Murakami, T. Kanezaki, Y. Mine and S. Matsuoka, Hydrogem embrittlement mechanism in fatigue of austenitic stainless steels, Metall Mater Trans 39A (2008) 1327-1339.
146. T. Kanezaki, C. Narazaki, Y. Mine, S. Matsuoka and Y. Murakami, Effects of hydrogen on fatigue crack growth behavior of austenitic stainless steels, Int J Hydrogen Energy 33 (2008) 2604-2619.
147. Y. Mine, C. Narazaki, K. Murakami, S. Matsuoka and Y. Murakami, Hydrogen transport in solution-treated and pre-strained austenitic stainless steels and its role in hydrogen-enhanced fatigue crack growth, Int J Hydrogen Energy 34 (2009) 1097-1107.
148. C. Skipper, G. Leisk, A. Saigal, D. Matson and C. San Marchi, Effect of internal hydrogen on fatigue strength of type 316 stainless steel, in: Somerday BP, Sofronis P and Jones R, editors, Effects of Hydrogen on Materials, Proceedings of the 2008 International Hydrogen Conference (Moran WY, 2008), ASM International, Materials Park OH, 2009, pp. 139-146.

149. K. Murakami, T. Kanezaki and Y. Mine, Hydrogen effect against hydrogen embrittlement, Metall Mater Trans 41 (2010) 2548-2562.
150. C. San Marchi and B.P. Somerday, Fatigue crack growth of structural metals for hydrogen service (PVP2011-57701), in: Proceedings of PVP-2011: ASME Pressure Vessels and Piping Division Conference (Baltimore MD, 2011), ASME,17-21 July 2011,
151. C. San Marchi, D.K. Balch, K. Nibur and B.P. Somerday, Effect of high-pressure hydrogen gas on fracture of austenitic steels, J Pressure Vessel Technol 130 (2008) 041401.
152. T.L. Anderson, Fracture Mechanics: Fundamentals and Applications (Third Edition), CRC Press, Boca Raton FL, 2005.

Table 1. Average hydrogen diffusivity and hydrogen solubility relationships for AISI type 300-series austenitic stainless steels.

Temperature range (K)	Hydrogen diffusivity $D = D_o \exp(-H_D / RT)$		Hydrogen solubility $K = K_o \exp(-\Delta H_s / RT)$		Ref.
	D_o $\left(\frac{\text{m}^2}{\text{s}}\right)$	H_D $\left(\frac{\text{kJ}}{\text{mol}}\right)$	K_o $\left(\frac{\text{mol H}_2}{\text{m}^3 \cdot \sqrt{\text{MPa}}}\right)$	ΔH_s $\left(\frac{\text{kJ}}{\text{mol}}\right)$	
423-700	6.6×10^{-7}	54.0	179	5.9	[34]
473-703	5.8×10^{-7}	53.6	488	8.6	[36]
373-623	2.0×10^{-7}	49.3	266	6.9	[35]

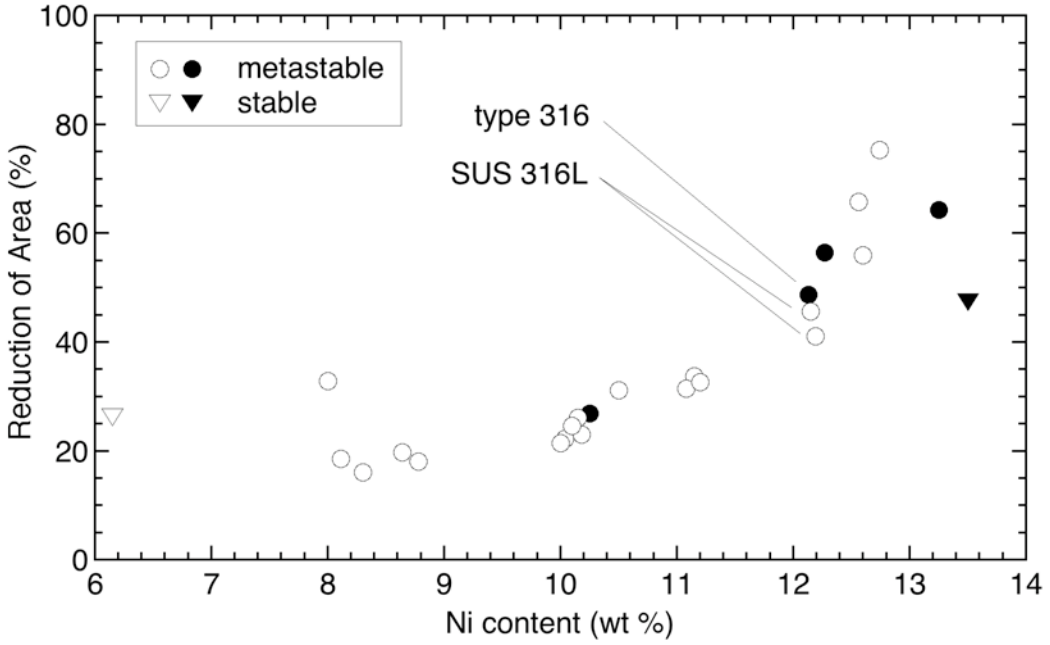

Figure 1. Reduction of area as a function of nickel content for a variety of thermally hydrogen-precharged metastable and stable austenitic stainless steels. Data from tensile testing at temperature of 223 K [66, 73]. Open symbols represent annealed materials; closed symbols represent strain-hardened material.

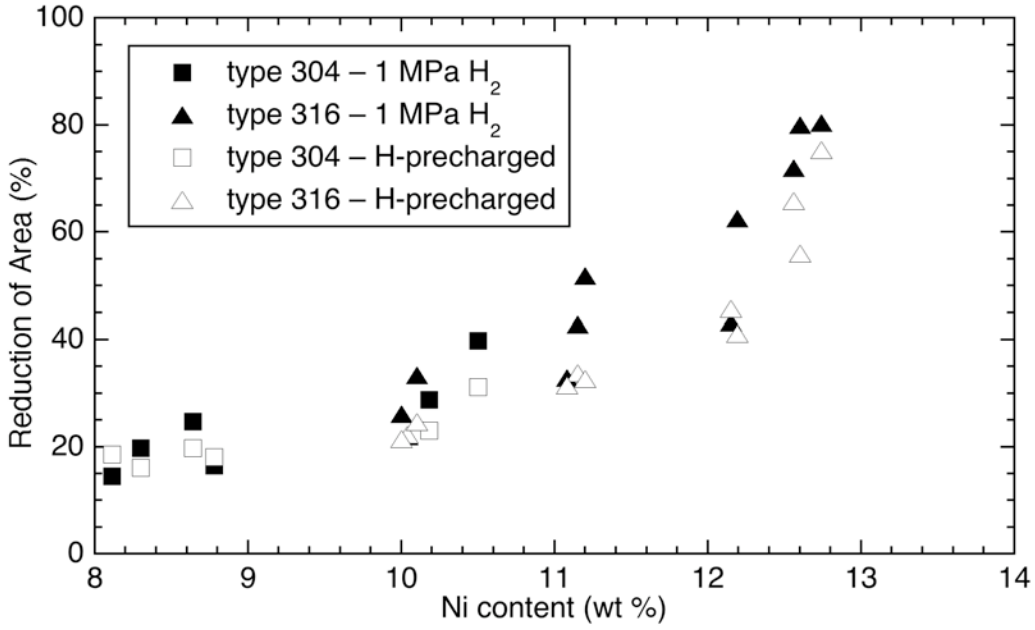

Figure 2. Reduction of area as a function of nickel content for a variety of AISI type 304 and AISI type 316 austenitic stainless steels. Data from tensile testing at temperature of 223 K [66].

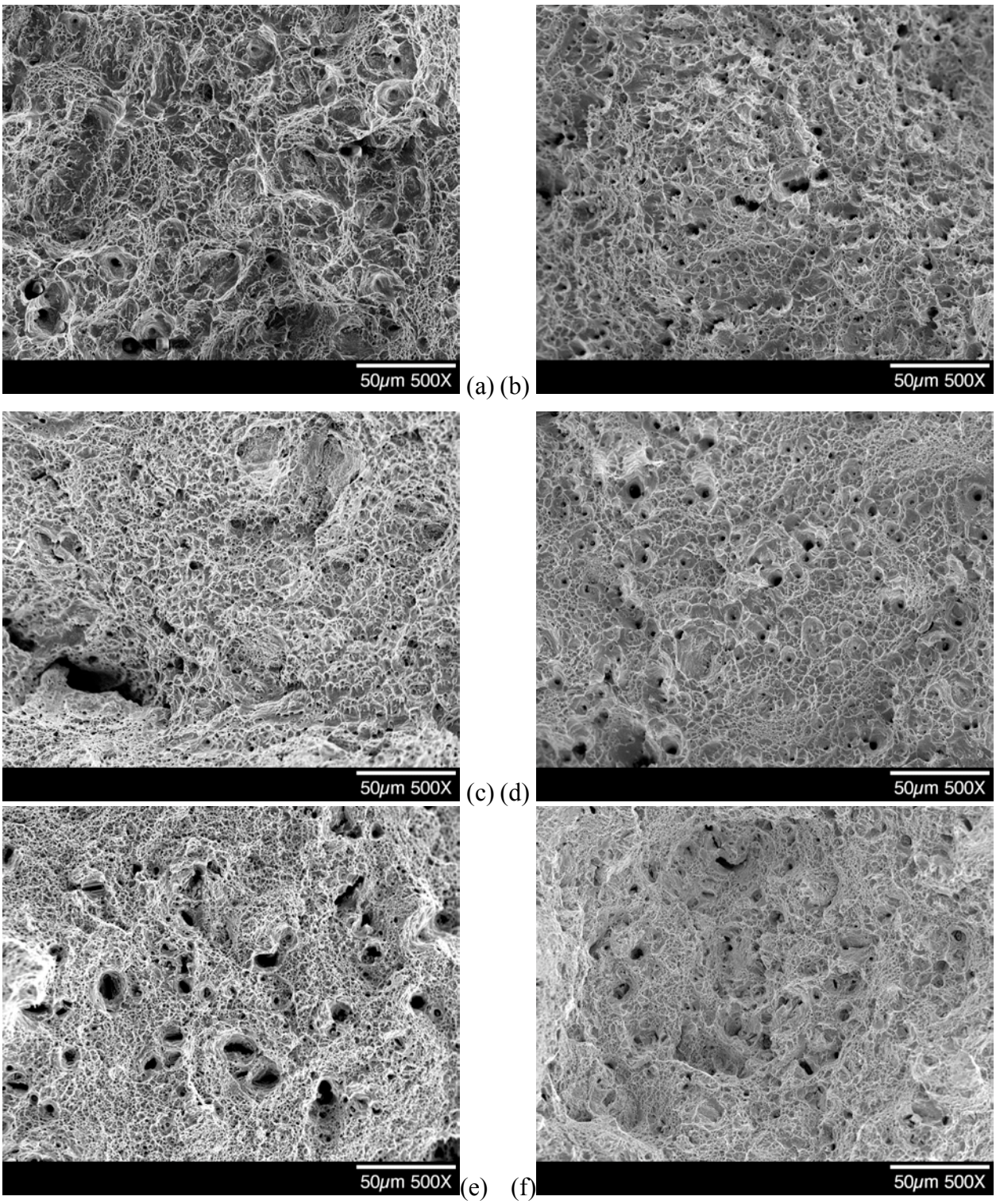

Figure 3. Fracture surfaces of thermally hydrogen-precharged austenitic stainless steels that display microvoid coalescence at room temperature. (a) 21Cr-6Ni-9Mn, annealed; (b) AISI type 316, annealed; (c) AISI type 316L, strain-hardended; (d) AISI type 316L, annealed; (e) 22Cr-13Ni-5Mn, forged; and (f) 22Cr-13Ni-5Mn, strain-hardened.

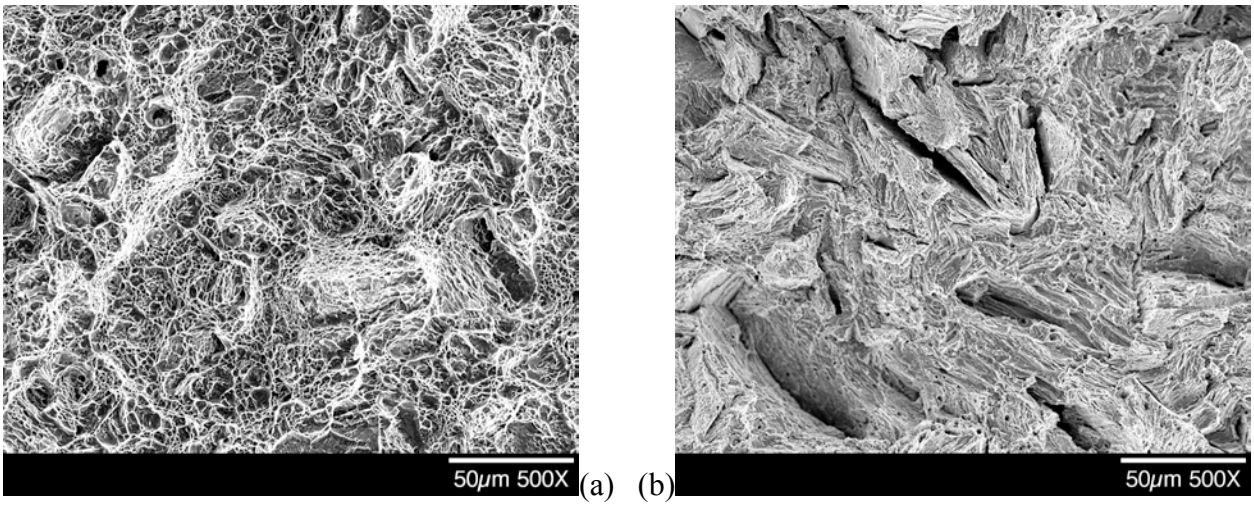

(a) (b)

Figure 4. Fracture surfaces of thermally hydrogen-precharged austenitic stainless steels that display elongated microvoid coalescence at room temperature. (a) 21Cr-6Ni-9Mn, forging; (b) AISI type 316, strain-hardened.

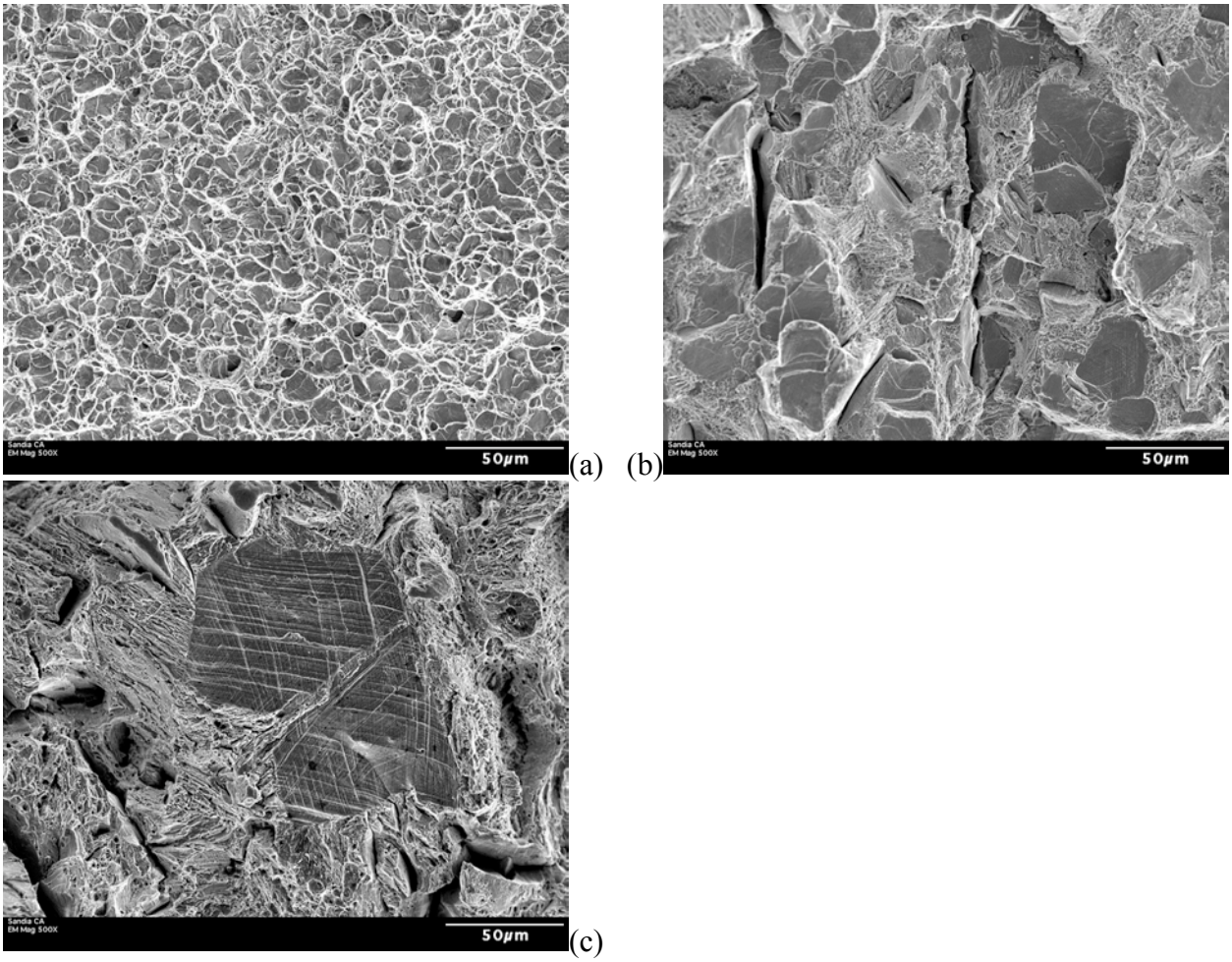

Figure 5. Fracture surfaces of thermally hydrogen-precharged austenitic stainless steels that display interface fracture at temperature of 223 K. The different size scale of the facets represents the relative size scale of the microstructure. (a) small, flat facets are separated by areas of MVC: 21Cr-6Ni-9Mn, annealed; (b) AISI type 304, annealed; and (c) AISI type 316L, strain-hardened.

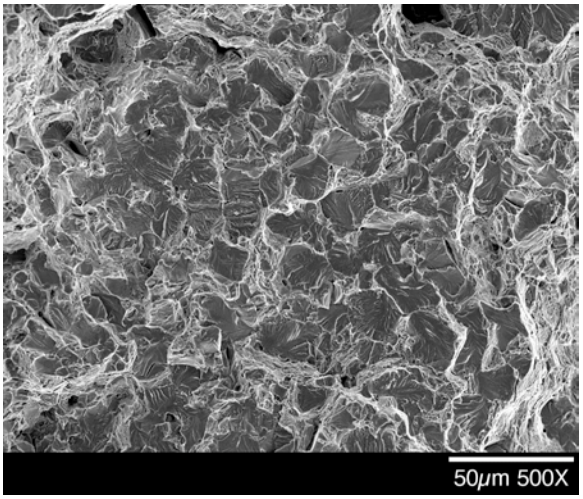

Figure 6. Fracture surface of duplex austenitic stainless steel (2507) that displays cleavage-like fracture in the ferritic phase and MVC in the austenitic phase between ferrite grains.

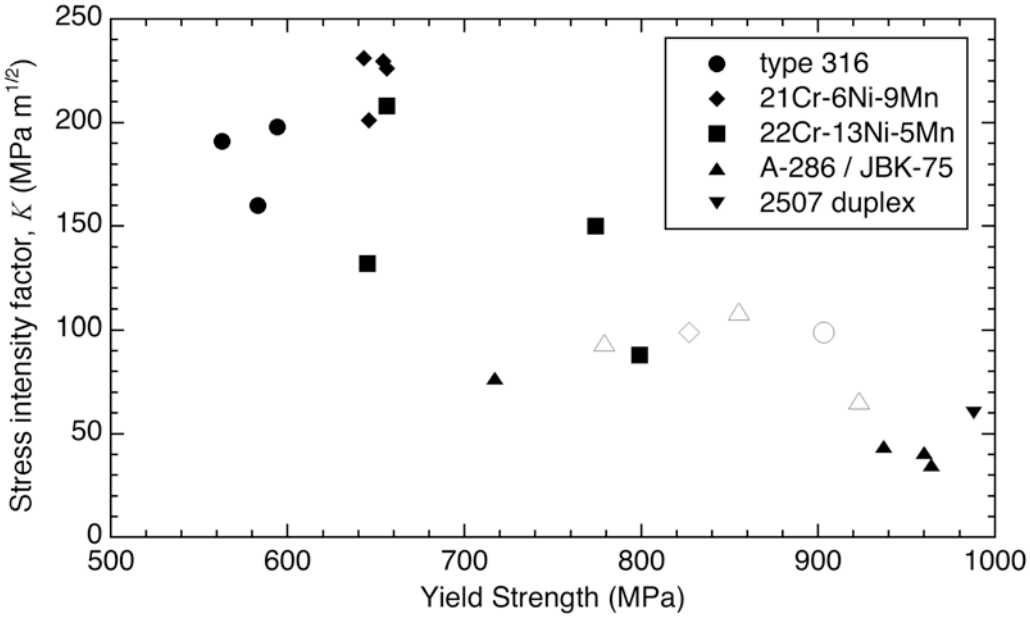

Figure 7. Stress intensity factor as a function of yield strength for a variety of austenitic stainless steels. Closed symbols represent elastic-plastic fracture toughness from thermally hydrogen-precharged materials [70, 73, 74, 140]; open symbols represent crack arrest threshold fracture toughness in gaseous hydrogen at pressure of 100 MPa [67].